Am J Cancer Res 2024;14(1):52-72
www.ajcr.us /ISSN:2156-6976/ajcr0152081

Original Article

Polydatin ameliorates low-density lipoprotein cholesterol and lipid metabolism by downregulating proprotein convertase subtilisin/kexin type 9 (PCSK9) in triple-negative breast cancer with hyperlipidemia

Min Liu[1], Qing Zhang[2]

[1]*School of Traditional Chinese Medicine, Capital Medical University, Beijing 100069, China;* [2]*Department of Oncology, Beijing Hospital of Traditional Chinese Medicine, Capital Medical University, Beijing 100010, China*

Received July 7, 2023; Accepted December 15, 2023; Epub January 15, 2024; Published January 30, 2024

Abstract: To investigate polydatin's effects on low-density lipoprotein cholesterol (LDL-C) and lipid metabolism in mice with triple-negative breast cancer (TNBC) and hyperlipidemia, as well as the underlying mechanism of proprotein convertase subtilisin/kexin type 9 (PCSK9). *In vivo*, we designed two animal models, namely breast pad *in situ* inoculation of TNBC model and TNBC with lung metastatic were inoculated with the caudal vein model. Mice were administered a high-fat diet. Upon the completion of the experiment, plasma triglycerides (TG), total plasma cholesterol (TC), plasma LDL-C, and plasma high-density lipoprotein cholesterol (HDL-C) were measured. ELISA was employed to measure PCSK9 and the low-density lipoprotein receptor (LDLR). The morphological alterations were observed using Oil-red O staining. Immunohistochemical labeling was used to determine the expression of PCSK9 and LDLR in mouse breast cancer (BC) tissues. MTT, wound healing assay, and the transwell migration and invasion test were conducted to examine co-cultured adipocytes' effects on the growth, invasion, and migration of BC cells. In the 4T1-luc cell model injected *in situ* into the breast pad and 4T1-luc cell model injected into the tail vein, we observed that a high-fat diet promoted the proliferation and lung metastasis of BC cells, whereas polydatin suppressed the proliferation and lung metastasis of BC cells. Co-culture of BC cells with adipocytes enhanced the proliferation, invasion, and metastasis, while polydatin intervention inhibited the growth, invasion, and metastasis. After treatment with polydatin, serum lipid levels decreased, PCSK9 decreased, LDLR increased, and LDL-C decreased in mouse BC, liver, and lung tissues. After polydatin treatment, PCSK9 decreased, LDLR increased, and LDL-C decreased in an *in vitro* co-culture system of BC cells and adipocytes. After transfection of siRNA PCSK9 in the co-culture system, the LDLR increased more significantly, and the LDL-C decreased more significantly. After transfection of LV-PCSK9, PCSK9 decreased, LDLR increased, and LDL-C decreased. We concluded that polydatin inhibited breast tumor proliferation and distant lung metastasis in mice promoted by a high lipid environment. By suppressing PCSK9, polydatin alters the lipid profile of hyperlipidemic TNBC mice and prevents distant metastases. Our findings provide credence to the established practice of using polydatin in treating TNBC combined with hyperlipidemia.

Keywords: Hyperlipidemia, polydatin, proprotein convertase subtilisin/kexin type-9 (PCSK9), triple-negative breast cancer (TNBC)

Introduction

The primary malignant tumor of the breast is breast cancer (BC). BC is the most common female malignant tumor, and its prevalence has been growing in recent years. BC is responsible for 11.7% of all cancer incidence and 6.9% of all cancer death [1]. BC without progesterone receptor (PR), human epidermal growth factor receptor 2 (HER-2), and the estrogen receptor (ER) are known as triple-negative BC (TNBC). Clinical therapy is challenging due to the lack of endocrine-targeted therapies. Additionally, BC-related metastasis is a primary cause of mortality.

Mammary adenocarcinoma formation and tumor growth are linked to fat-rich environ-

https://doi.org/10.62347/BRNK8140

ments [2]. One of the leading causes of BC is obesity [3]. Cancer-associated adipocytes (CAA) are considered to develop when cancer cells interact with adipocytes in the tumor microenvironment, and these adipocytes are important biological components of the BC microenvironment. Adipocytes were initially identified as a great energy reserve that delivers high-energy metabolites upon interaction with BC cells [4]. CAAs' metabolic reprogramming may be linked to their significant tumor-promoting capabilities. BC cells and CAAs interact dynamically, and it is thus speculated that tumors can induce the reprogramming of metabolic synergy in adipocytes and adapt to intracellular metabolic processes to support proliferation. Obesity and diet are critical risk factors for the emergence of BC. Cancer cells that are proliferating need more cholesterol. Low-density lipoprotein cholesterol (LDL-C) absorption from the circulation is increased in BC tissue through increased low-density lipoprotein receptor (LDLR) expression [5]. In contrast to ER-positive MCF-7 cells, MDA-MB-231 cells have higher LDLR gene and protein levels *in vitro* [6]. Accordingly, LDL-C can primarily enhance the proliferation and migration in ER-negative cells, although ER-positive cell lines did not exhibit this effect [7, 8]. Furthermore, it was shown that HER-2-positive breast cells were related to elevated plasma LDL-C levels [9]. Notably, the most aggressive BC subtypes are HER-2 positive and TNBC [10].

Proprotein convertases, like endoproteases subtilisin and kexin, are Ca^{2+}-dependent serine proteases. Proprotein convertase subtilisin/kexin type-9 (PCSK9), produced by the liver and other organs, binds to LDLR and promotes the trafficking of the receptor-LDL complex to the lysosomal compartment, where it is destroyed and total LDL levels are downregulated [11]. The relationship between PCSK9 and LDL-C levels was elucidated by defining PCSK9 mutation in patients with familial hypercholesterolemia [12]. The approval and commercialization of the humanized PCSK9 monoclonal (mAb) antibody medications, evolocumab and alirocumab, show that using mAbs to inhibit PCSK9-mediated LDLR breakdown may decrease LDL-C levels [13]. Reducing PCSK9 expression may reduce serum lipids and hence slow down the growth and recurrence of BC [14]. As a result, PCSK9 might be a promising target in alleviating lipid and lipid metabolism disorders and suppressing BC cell activity.

One primary active ingredient of *Polygonum cuspidatum Sieb*. et Zucc is polydatin (resveratrol-3-O-mono-D-glucoside). It is a resveratrol glycoside. Polydatin has been demonstrated in previous research to have numerous pharmacological actions, including anti-inflammatory [15, 16], anti-oxidant [17-19], anti-allergy [20], anti-cancer [21-24], lipid-lowering [25], and cardiovascular protective [26] activities. We discovered that polydatin might enhance lipid metabolism in TNBC [27]. Polydatin's effect on PCSK9 and LDLR expression in high-fat diet (HFD)-fed mice TNBC has, however, been the subject of very few investigations. Given the intimate association between PCSK9 and LDLR, as well as lipid metabolism, this study aimed at investigating whether polydatin affects PCSK9 in TNBC.

We used a co-culture model of 4T1 cells and 3T3-L1 cells and a mouse model of tail vein metastasis with an HFD based on the aforementioned background to investigate the precise effects of polydatin on PCSK9 and LDLR in TNBC. To further elucidate its regulatory role in LDL-C, we knocked down and overexpressed the PCSK9 *in vitro*. Our findings show that polydatin can improve lipid metabolism in TNBC with an HFD via downregulating PCSK9. This finding will provide not only a lipid-lowering target for TNBC patients with hyperlipidemia, but also a new means of treatment.

Materials and methods

Chemicals and reagents

The chemicals were purchased from Sigma-Aldrich (St. Louis, MO, USA) unless otherwise indicated. Life Sciences (Carlsbad, CA, USA) provided cell culture reagents.

Cell lines and culture conditions

The American Type Culture Collection (ATCC, Rockville, MD, USA) provided the human BC cell line MDA-MB-231 and the mouse mammary cancer cell line 4T1-Luc. At 37°C in a humidified environment of 95% air and 5% CO_2, the cells were cultured in Dulbecco's modified Eagle's medium (DMEM, Gibco, USA) nourished with 10% fetal bovine serum (FBS) (Gibco). The MCF-

10A non-tumorigenic epithelial cells were provided by ATCC and were cultured in DMEM-F12 (Invitrogen, MA, USA) with 10% FBS (Gibco), 20 ng/mL EGF, 0.3 g/L l-glutamine, 40 mg/L gentamicin, 10 μg/mL insulin, and 500 μg/mL hydrocortisone. All cultures were kept at 37°C with 5% CO_2 in humidified atmosphere.

Culture and differentiation of 3T3-L1 preadipocytes

ATCC supplied 3T3-L1 pre-adipocytes. The cells were cultured in high glucose DMEM with 1% antibiotic solution and 10% bovine calf serum (BCS, Gibco-Invitrogen, USA) at 37°C in a humidified atmosphere with 5% CO_2. A cocktail technique was used for the purpose of inducing the differentiation of 3T3-L1 cells into mature adipocytes. A differentiation cocktail of 0.5 mM isobutyl methylxanthine (IBMX), 1 mM dexamethasone, and 10 g/mL insulin were added to cells 2 days after confluence (day 0), and then the cells were switched to a maintenance medium containing DMEM, 10 g/mL insulin, and 10% FBS. Every other day, the medium was replenished.

Co-culture

In a transwell system (0.4 m hole size, Corning, USA) of culture, 3T3-L1 pre-adipocytes or adipocytes were co-cultured with MDA-MB-231 cells. MDA-MB-231 (3×10^4/well) and 3T3-L1 pre-adipocytes or adipocytes (2×10^4/chamber) were seeded into 6-well culture chambers and culture plates, respectively. Then, MDA-MB-231 cells were transfected with PCSK9 siRNA and lentiviral vector after 12 h. DMEM with 1% FBS was used after 8 h. Finally, we co-cultured implants in six-well plates.

Cell transfection

Guangzhou Ribobio Co., Ltd. (Guangzhou, China) provided the PCSK9 siRNA. The PCSK9 small interfering (siRNA) candidate sequence was GAGGTGTATCTCCTAGACA. The negative control sequence was CCCATGTCGACTACATCGA. After dissolving the siRNAs in RNase-free sterile water, they were diluted to a 20 M sock solution and kept at -20°C. The 50 nM PCSK9 siRNA or 50 nM scrambled siRNA (Ribobio) was transfected into the cells in a 2 mL transfection solution using riboFECT CP Reagent. After that, we co-cultured the inserts on 6-well plates. The cells were obtained from the co-culture after 48 h.

GeneChem Co., Ltd. (Shanghai, China) created the PCSK9 lentiviral vector. The PCSK9 lentiviral vector carrying the scrambled sequence was used as a negative control. The multiplicity of infection (MOI) = 10 was used for transfection, with an MOI estimate obtained from a pilot study. In a 1 mL complete medium with 40 μL of Hitrans G P infection reagent, the PCSK9 and negative control lentiviral vectors were added. After 8 h, the lentiviral vector media was replaced with a new medium containing fresh serum. The inserts were subjected to co-culturing after being moved to 6-well plates. The cells were collected from the co-culture after 48 h.

In vitro studies

Experimental treatment: A final 1 mM stock solution of polydatin was created by dissolving it in dimethyl sulfoxide (DMSO), which was then used to create a treatment medium at different concentrations. Within a specific experiment, the final DMSO concentration was kept constant and never went beyond 0.1% in any of the treatment groups.

MTT cell proliferation assay: MDA-MB-231 cells' viability in the co-culture system was determined by means of the quintuplicate MTT assay. After co-culturing 3T3-L1 pre-adipocytes or adipocytes, each well received 500 μL of MTT (5 mg/mL, Progema, Madison, WI, USA). Incubation continued for 4 hours. Each well received 3.75 mL DMSO. The absorbance of each well was measured daily at 492 nm using a microplate reader to generate a growth curve. The experiment was conducted thrice.

Wound-healing assay: MDA-MB-231 cell migration was examined by wound-healing assay. A sterile 10 μL pipette tip was used to wound the cell monolayer at 80% confluence. A light microscope was used to photograph cell movement at 0, 24, 48, and 72 h after co-culturing. The percentage of healing was calculated as follows: (width at 0 h - width at 24 h/48 h/72 h)/width at 0 h × 100%. Three separate assays were conducted.

Transwell migration assay: After two days of co-culturing, MDA-MB-231 cells with 3T3-L1 pre-adipocytes or adipocytes, migration experi-

ments were conducted. In 0.4 mL, 2 × 10^5 MDA-MB-231 cells were co-cultured in a serum-free media. The cell suspension was transferred to the top chamber after the co-culture system's medium containing 10% FBS was introduced into the bottom chamber as a chemoattractant. The cells were rinsed twice with phosphate-buffered saline (PBS) after being fixed in 4% paraformaldehyde for 24 h and stained with crystal violet for 30 min. A light microscope with a magnification of ×100 was used to view the migrating cells. The means of five fields per well were calculated. The procedure was repeated three times.

Oil red staining: Adipocytes were washed twice in PBS (pH value, 7.4) after 30 min exposure to 4% paraformaldehyde. Each well received 1.5 mL of Oil red staining solution before incubation for 30 min. Cells were microscope-analyzed after two PBS washes.

In vivo studies

Animals: In the current investigation, 8-week-old female BALB/c mice (Beijing HFK Bioscience Co., Ltd., Beijing, China) were used. Experiments were performed under a project license granted by ethics board of Beijing Viewsolid Biotechnology Co., Ltd. (No. 202000038). All animals were housed in typical laboratory conditions at the Beijing Hospital of Traditional Chinese Medicine (22-24°C, 40%-60% relative humidity, 12/12-hour light/dark cycle) with an unlimited supply of water and food. The mice were sacrificed using cervical dislocation euthanasia method. All experimental procedures followed the Guidance for the Care and Use of Laboratory Animals from the Ministry of Science and Technology of China.

Polydatin's in vivo effects on TNBC growth and metastasis in a 4T1 breast tumor-bearing mouse model: Six female BALB/c mice were randomly assigned to vehicle control and polydatin treatment groups. Daily intraperitoneal injections of 100 mg/kg polydatin or vehicle control was begun one week before xenografting tumor cells and continued until the end of the experiment. Under anesthesia, 1 × 10^5 4T1 cells/50 μL were xenografted subcutaneously to the right fourth mammary fat pad of each mouse. Tumor growth at the injection site in mice was monitored daily. After 7 days, a 50 mm^3 tumor formed. Vehicle-treated control mice had tumors with an average volume of 1000 mm^3 after 28 days. Tumors from both groups of animals were collected and frozen at -80°C. Animals initially given vehicle control therapy continued receiving that medication after the removal of primary breast tumors. However, mice administered polydatin treatment received the same intraperitoneal injection of 100 mg/kg for an additional 10 days. Mice were then sacrificed at specified intervals unless they seemed moribund or had tumor volumes >1500 mm^3, in which cases they were sacrificed immediately. A digital caliper was used to measure the tumor size every two days. The standard formula for calculating tumor volume is as follows: tumor volume (mm^3) = [(length × $width^2$)/2]. After the experiments were complete, the mice were sacrificed, and their blood was collected in heparin-treated microtiter tubes and centrifuged for 15 min at 4°C and 13000 rpm to separate the plasma. The plasma samples were stored at -80°C for further measurement of PCSK9/LDLR, triglycerides (TG), total cholesterol (TC), high-density lipoprotein cholesterol (HDL-C), and LDL-C. Collected tumors and organs were weighted and preserved at -80°C until total protein extraction for WB analysis.

Tail vein metastasis assays: Mature adipocyte differentiation was induced in 3T1-L1 cells. Then, polydatin was applied alone each day when co-culturing 4T1-luc cells and 3T3-L1 cells. Following treatment, mice (n = 6 per group) were intravenously injected with 1 × 10^6 4T1-luc cells. Tumors were allowed to grow for a week. Then, the mice were executed, and lung tissues were taken for analysis.

Assessment of polydatin effects on the TG, TC, HDL-C, and LDL-C

Per the manufacturer's instruction, TC, TG, HDL-C, and LDL-C test kits (Nanjing Jiancheng Bioengineering Institute, Nanjing, China) were used to examine samples from both vehicle-treated and polydatin-treated mice.

Assessment of polydatin effects on the LDLR and PCSK9 levels in serum

Serum PCSK9 and LDLR levels were assessed in polydatin-treated and vehicle control mice using PCSK9 (Abcam, USA) and LDLR ELISA kit (LSBio, USA), following the manufacturer's instructions.

Hematoxylin and eosin (H&E) staining

H&E stain was performed on 10% neutral formalin-fixed paraffin-embedded tissue slices, as it is a standard technique. The sections were deparaffinized quickly, rehydrated, stained with hematoxylin and stirred for 20 s, stained with 1% eosin, and rinsed with water for 15 s, dehydrated, and covered with neutral balsam.

Immunohistochemistry (IHC)

The tissue sections were sectioned into 5 m thick slices after being fixed in 10% formalin for 24 hours and then embedded in paraffin. Tissue slices were deparaffinized three times for 5 min each, washed three times for 5 min each with distilled water, and rehydrated in a descending ethanol series (100% 5 min, 95% 5 min, 70% 5 min, 50% 5 min, and 30% 5 min). The tissue slices were cooled for 30 min on a bench and then incubated with 3% H_2O_2 for 10 min after being rinsed with distilled water. Using 1X Tris-buffered saline, tissue sections were washed, followed by 1.5-hour incubation at room temperature (RT) in Tris-buffered saline with 0.1% Tween 20 (TBST) and 10% normal goat serum. Tissue slices were treated with primary antibodies diluted 1:250 against PCSK9 and LDLR overnight at 4°C. Following three washes in TBST buffer, tissue slices were incubated in a boost IHC detection reagent for 30 min at room temperature. After a wash in buffer, we used a DAB detection kit and polymeric detecting equipment per the manufacturer's recommendations. Hematoxylin was then used as a counterstain for 1 min at the tissue slices. Sections were dehydrated using 95% ethanol, absolute ethanol, and xylene. Finally, sections were coverslipped with mounting media.

Tumor visualization using an in vivo imaging system (IVIS)

Mice were photographed weekly using the Xenogen IVIS Spectrum IVIS to detect tumor progression and metastasis. They were weighed, injected intraperitoneally with 150 mg/kg of 15 mg/mL luciferin, and anesthetized with 2.5% isoflurane. Then, their luminescence at 10 min was measured using the IVIS. Luminescence was measured by identifying a region of interest (ROI) and calculating its average radiance with the aid of Perkin Elmer's (Cheshire, UK) Living Image software. The signals from each animal were then compared using ROI.

Western blotting (WB)

RIPA buffer (Med Chem Express, USA) containing 50 mM Tris-HCl (pH 7.5), 0.1% SDS, 1% NP-40, 150 mM NaCl, and a protease inhibitor cocktail was used to homogenize cells or tissues of each group. The resulting whole-cell lysates were analyzed by WB.

As previously mentioned, WB's routine procedures were followed. The samples were incubated with primary antibodies, including rabbit anti-PCSK9 antibody (1:1000, Abcam, USA), rabbit anti-LDLR antibody (1:1000, Abcam, USA), mouse β-actin mAb (1:5000, ProteinTech, USA), and rabbit anti-LDL-C antibody (1:1000, Abcam, USA). Incubation with Dylight 680- or 800-labeled secondary antibody (1:10000) for 1 h was conducted after three washes with TBST to remove unbound secondary antibody. Odyssey version 3.0 (LI-COR Biosciences) was used to identify the relative protein band density. Image-Pro Plus Version 6.0 (Media Cybernetics, Inc., Rockville, USA) was used to measure the signal intensity.

RNA isolation and RT-PCR

Tissues and cells from co-cultured MDA-MB-231 were extracted using Trizol reagent (Invitrogen, Carlsbad, CA, USA) as per the manufacturer's instructions. Following reverse transcription using a Primer Script Kit, 1 gram of total RNA was used to amplify cDNA (TaKaRa, Dalian, China). The expression of the mRNA for the target genes was normalized concerning that of β-actin or GAPDH, as applicable. The primers in this study are listed in **Table 1**.

Statistics

The results of at least two independent investigations are presented as mean ± standard error of the mean (SEM). The differences between two groups were analyzed using the Student's two-tailed t-test (control vs. treatment). One-way analysis of variance (ANOVA) was used to compare among three or more groups (control vs. different treatment concentration groups), and Dunnett's test was used for post hoc analysis. All statistics were generated using GraphPad Prism version 8 (La Jolla,

Table 1. Primers sequences

Genes		Sequences (5'-3')	Species
PCSK9	Sense	5'-AGGGGAGGACATCATTGGTG-3'	*Homo sapiens*
	Antisense	5'-CAGGTTGGGGGTCAGTACC-3'	
LDLR	Sense	5'-CAATGTCTCACCAAGCTCTG-3'	*Homo sapiens*
	Antisense	5'-TCTGTCTCGAGGGGTACCTG-3'	
β-actin	Sense	5'-AGGGGCCGGACTCGTCATACT-3'	*Homo sapiens*
	Antisense	5'-GGCGGCACCACCATGTACCCT-3'	
PCSK9	Sense	5'-TTGCAGCAGCTGGGAACTT-3'	*Mus musculus*
	Antisense	5'-CCGACTGTGATGACCTCTGGA-3'	
LDLR	Sense	5'-ACCTGCCGACCTGATGAATTC-3'	*Mus musculus*
	Antisense	5'-GCAGTCATGTTCACGGTCACA-3'	
β-actin	Sense	5'-TGCGTGACATCAAAGAGAAG-3'	*Mus musculus*
	Antisense	5'-GATGCCACAGGATTCCATA-3'	
PPAR-γ	Sense	5'-ACCAAAGTGCAATCAAAGTGGA-3'	*Homo sapiens*
	Antisense	5'-ATGAGGGAGTTGGAAGGCTCT-3'	
C/EBP-α	Sense	5'-TATAGGCTGGGCTTCCCCTT-3'	*Homo sapiens*
	Antisense	5'-AGCTTTCTGGTGTGACTCGG-3'	
FABP4	Sense	5'-ACTGGGCCAGGAATTTGACG-3'	*Homo sapiens*
	Antisense	5'-CTCGTGGAAGTGACGCCTT-3'	
HSL	Sense	5'-AGGAGCCAGCATTGAGACAAA-3'	Homo sapiens
	Antisense	5'-CGCAGGTGTTGATTCAGCTTC-3'	
PREF1	Sense	5'-CTTTCGGCCACAGCACCTAT-3'	*Homo sapiens*
	Antisense	5'-TGTCATCCTCGCAGAATCCAT-3'	
GAPDH	Sense	5'-AGGTCGGTGTGAACGGATTTG-3'	*Homo sapiens*
	Antisense	5'-TGTAGACCATGTAGTTGAGGTCA-3'	

CA, United States). Statistically significant differences were denoted by *P<0.05, **P<0.01, and ***P<0.001 relative to the vehicle-treated control group.

Results

Formation and identification of CAAs

3T3-L1 and MDA-MB-231 cells were co-cultured to study how adipocytes affect TNBC in the tumor microenvironment. Pre-adipocytes 3T3-L1 were inoculated in cell culture dishes for culture (**Figure 1A**). With the progress of cell culture, when the growth fusion rate of pre-adipocytes 3T3-L1 reached 100%, the contact inhibition of cell growth showed a scroll growth (**Figure 1B**). After 15 days of induction, the majority of the pre-adipocytes 3T3-L1 were induced into mature adipocytes, the shape of adipocytes progressively rounded out, and the quantity and volume of lipid droplets in the cytoplasm increased (**Figure 1C**). Mature fat cells' cytoplasm might be stained red by lipid droplets, according to oil red O staining (**Figure 1D**). The q-PCR results revealed that mature adipocytes up-regulated C/EBP-α, fatty acid binding protein 4, and PPAR-γ expression but down-regulated pre-adipocyte factor 1 and hormone-sensitive lipase (HSL) expression (**Figure 1E**), indicating that pre-adipocytes have been induced to undergo differentiation into mature adipocytes.

TNBC cells were then grown with either pre- or mature adipocytes. Because the hole size of the Transwell chamber used was just 0.4 m, the adipocytes were not in physical contact with the TNBC cells (**Figure 2A**). Adipocytes co-cultured for 24 h had lower C/EBP-α and PPAR-γ expression and higher HSL expression than untreated adipocytes (**Figure 2B**). These findings imply that TNBC cells had no significant effect on pre-adipocytes. Oil red O staining revealed that adipocyte lipid droplets were densely packed, although co-cultured adipocyte lipid droplets were widely dispersed and smaller in volume (**Figure 2C**, **2D**). The finding

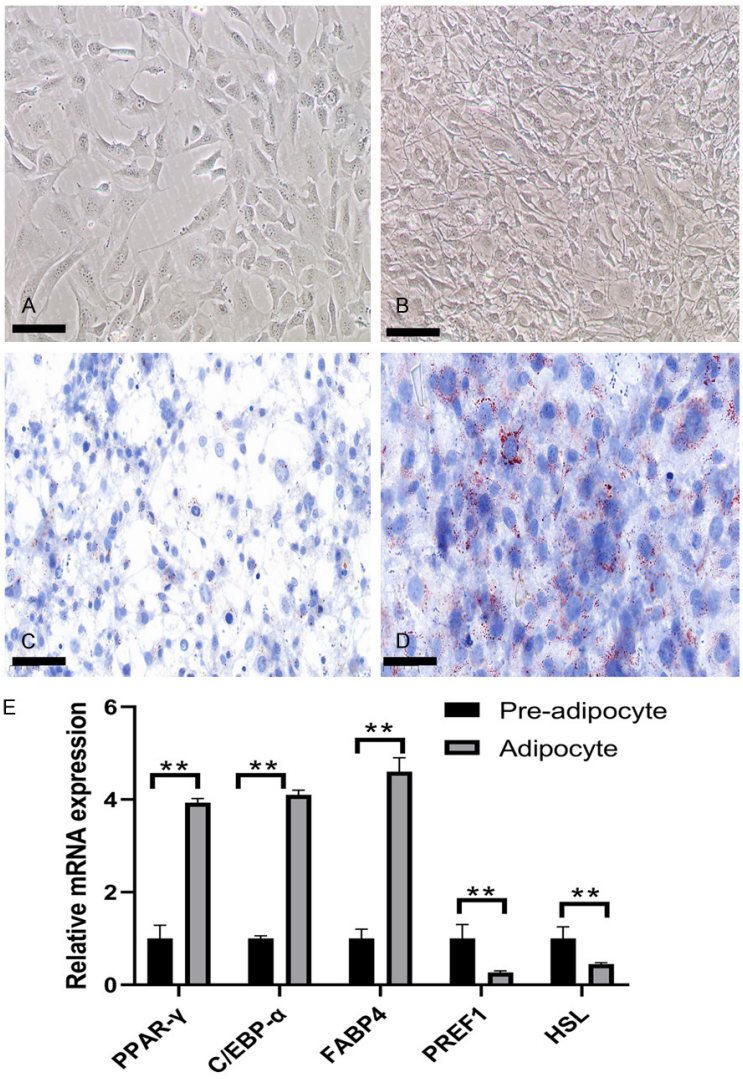

Figure 1. 3T3-L1 pre-adipocytes were induced to differentiate into mature adipocytes. A. Pre-adipocytes 3T3-L1 cells in culture. B. Pre-adipocytes 3T3-L1 cells were in a contact inhibition state. C. Mature adipocytes. D. Oil red O stained mature adipocytes, scale bar: 100 μm. E. In pre-adipocytes and mature adipocytes, q-PCR was used to examine the mRNA expression of differentiation markers. An illustration of typical microscopic fields is displayed, and quantitative data from at least three different experiments are presented as mean ± SD. **P<0.01.

mentioned above indicates that the adipocytes transformed into CAAs after being co-cultured with TNBC cells.

In a tail vein metastatic mouse model, an HFD aided 4T1 TNBC lung metastasis

In the prior investigation, we discovered that an HFD accelerated 4T1 TNBC development in a breast tumor-bearing mouse model [27]. An HFD model had been successfully established when the lipid phase index in mice was raised. Compared to the regular chow diet group, BALB/c mice fed with an HFD exhibited elevated serum levels of TC, TG, LDL-C, and HDL-C (**Figure 3A-D**).

On the seventh day post-inoculation, a notable reduction in the body weight of mice prompted us to collect samples. Specifically, the mice belonging to the tumor-bearing with lung metastasis mouse model group (N-Tumor) was higher than that of the black control group (N-Con). The group of mice subjected to an HFD exhibited a greater lung weight (**Figure 3E**, **3F**). Based on the aforementioned findings, it can be inferred that an HFD potentially facilitated the occurrence of 4T1 TNBC lung metastasis in mouse model specifically designed to simulate tail vein metastasis.

Polydatin decreased the effect of CAAs on TNBC proliferation, invasion, and migration in vitro

The impact of polydatin on the proliferation of TNBC cells in a co-culture system was investigated using the MTT assay (**Figure 4A**).

Next, we assessed the lateral migratory capacity of TNBC cells using a wound healing assay. In comparison to the positive control group, the PD group exhibited a significant reduction in cellular migration ability (**Figure 4B**, **4D**).

The longitudinal migratory capacity of TNBC cells was assessed using the Transwell invasion and migration assay. Similarly, compared to the positive control group, the PD group exhibited a significant reduction in both invasive and migratory abilities (**Figure 4C**, **4E**).

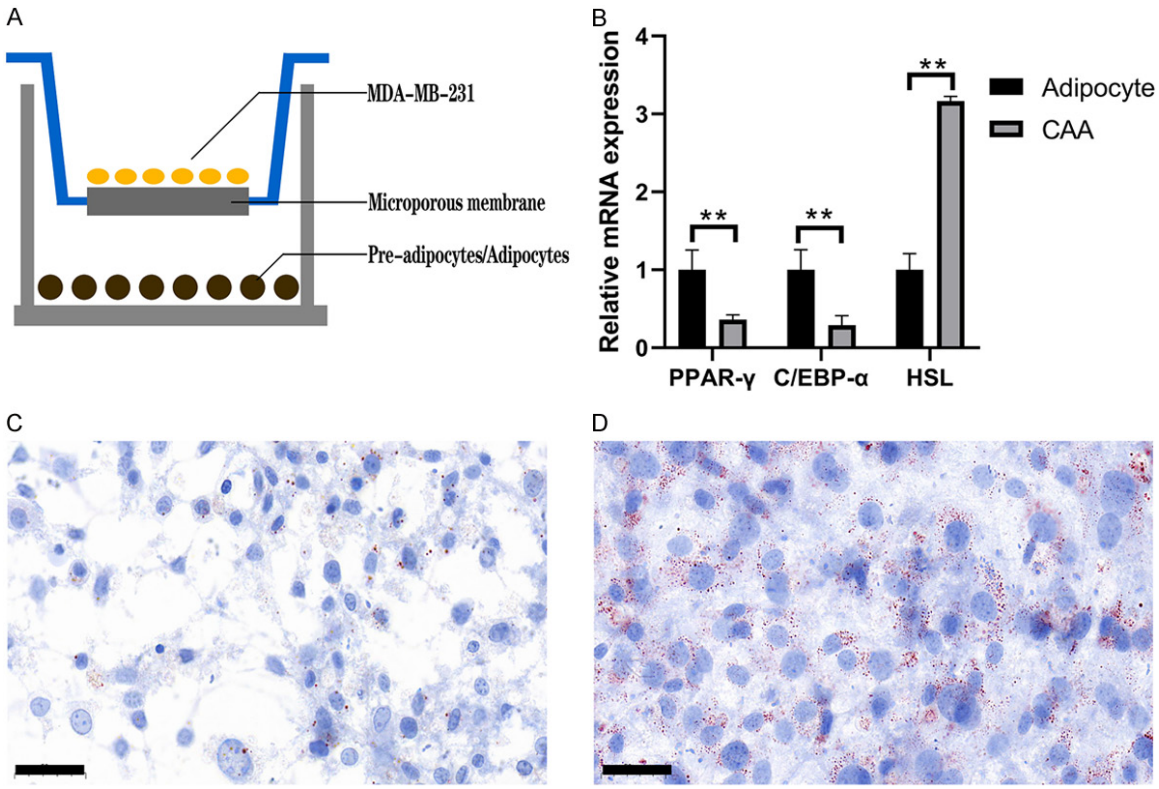

Figure 2. Cancer-associated adipocyte formation. A. Co-culture model of TNBC cells and adipocytes. B. In adipocytes and CAAs, q-PCR was conducted to measure the mRNA expression of differentiation markers. C. Adipocytes, scale bar: 100 μm. D. CAAs, scale bar: 100 μm. Quantitative results from at least three experiments are presented as mean ± SD with an illustration of typical microscopic fields. **P<0.01.

These data suggest that polydatin exhibits potential inhibitory effects on the invasion and migration of TNBC cells in a co-culture system.

Polydatin decreased the impact of CAAs on TNBC expansion and metastasis in vivo

In the breast tumor-bearing mouse model, our study revealed that the administration of polydatin effectively impeded the progression of TNBC and inhibited lung metastasis [27]. The levels of TC, TG, LDL-C, and HDL-C in the plasma of mice from N-Con group, N-Tumor group, and N-PD group exhibited comparable values (**Figure 5A-D**). These findings indicate that the consumption of polydatin does not have any discernible impact on the blood lipid profile of mice fed with a regular chow diet.

After establishing a mouse HFD model, we utilized polydatin to assess the lipid profile of HFD-fed mice. Compared to the N-Con group, the H-Con and H-Tumor groups exhibited elevated levels of LDL-C, TG, and TC, while HDL-C levels were decreased. Conversely, the H-PD group demonstrated higher HDL-C content compared to both the H-Con and H-Tumor groups, along with lower levels of LDL-C, TG, and TC (**Figure 5E-H**). These findings indicate that polydatin exerts a direct impact on reducing blood lipids in HFD-fed mice.

Next, distant lung metastasis was observed in TNBC mice after an HFD. Additionally, samples were collected on day 7 post-inoculation. The lung weight of mice in the HFD group was significantly higher than that in the control group fed with an ordinary diet, whereas treatment with polydatin resulted in a reduction in lung weight (**Figure 5I**). These results demonstrate that polydatin effectively attenuates the impact of CAAs on the progression and metastasis of TNBC *in vivo*.

Polydatin suppressed the combination of PCSK9-LDLR and inhibited the expression of LDL-C in vivo

The expression of PCSK9 protein and mRNA were significantly upregulated in mammary

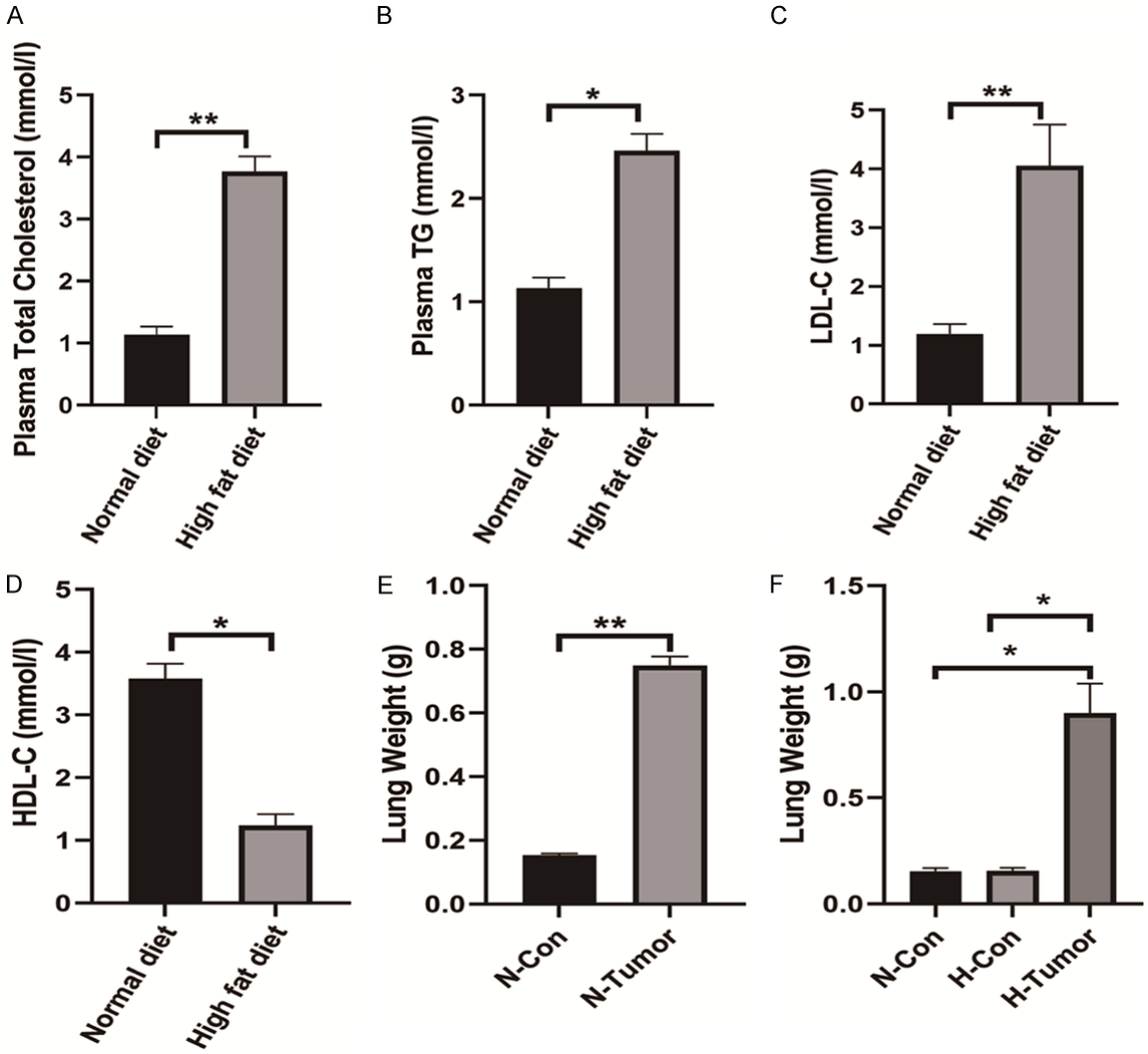

Figure 3. Successful establishment of a high-fat diet (HFD) model. A. The plasma total cholesterol (TC). B. The plasma triglyceride (TG). C. The plasma low-density lipoprotein cholesterol (LDL-C). D. The plasma high-density lipoprotein cholesterol (HDL-C). The lung weight in a tail vein metastatic mouse model of 4T1 TNBC. E. The lung metastases in mice with TNBC with a standard chow diet. F. The lung metastases in mice with TNBC administered HFD. **P<0.01, *P<0.05. N-Con, the blank group with a standard chow diet; N-Tumor, tumor-bearing mice with a standard chow diet; H-Con, the blank group administered HFD; H-Tumor, tumor-bearing mice administered HFD.

tumors of mice, particularly in those fed an HFD (**Figure 6A-C**). The results of this study indicate that PCSK9 exhibits predominant expression in breast tumor tissues.

PCSK9 can mediate the degradation of LDLR and regulate plasma LDL-C levels. The expression of PCSK9 and LDLR after polydatin intervention were observed in mice because polydatin can reduce the lipid level (including LDL-C) of mice. The expressions of PCSK9 and LDLR in the 4T1 group and 4T1+polydatin group were detected using the IHC method in mouse mammary tumor tissues. The results showed that PCSK9 was substantially downregulated and LDLR was upregulated in the 4T1+polydatin group compared to those in the 4T1 group (**Figure 6D-F**). Serum PCSK9 and LDLR levels were determined by ELISA. The results demonstrated a significant upregulation of PCSK9 in tumor-bearing mice, and the HFD further augmented the expression of PCSK9. Polydatin exhibited a suppressive effect on PCSK9 expression, while LDLR displayed an inverse expression to PCSK9 (**Figure 6G**, **6H**).

Effect of polydatin on the expression of PCSK9 and LDLR in situ mammary tumor, lung, and

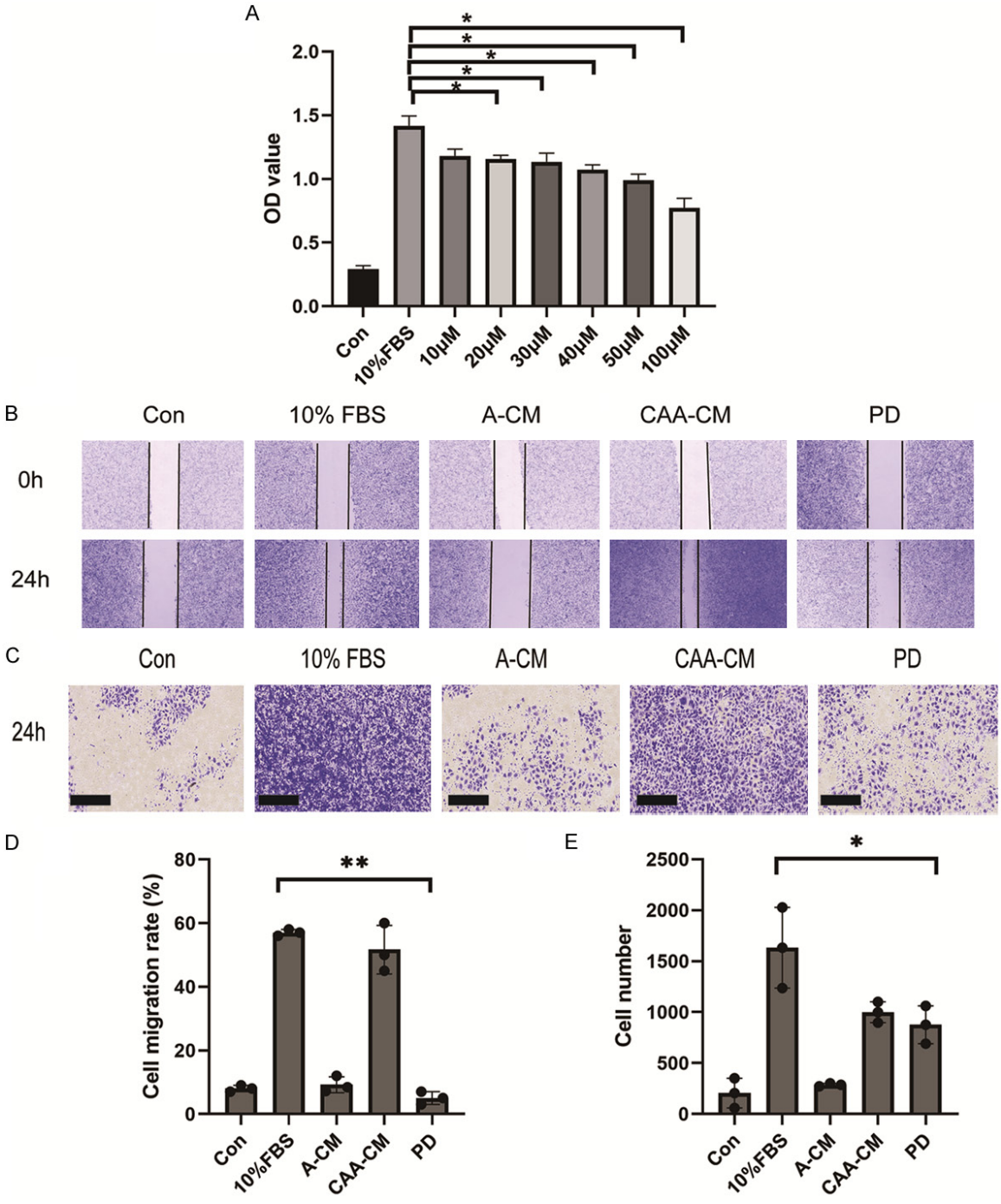

Figure 4. Polydatin's effect on TNBC cell proliferation, invasion, and migration in a co-culture system. (A) TNBC cell proliferation in a co-culture system. (B) Invasion of TNBC cell invasion in a co-culture system. (C) TNBC cell metastasis in a co-culture system, scale bar: 100 μm. (D, E) The statistical chart for (B) and (C). **P<0.01, *P<0.05. Con, negative control group; 10% FBS, positive control group; A-CM, conditioned medium for mature adipocytes; CAA-CM, conditioned medium from CAA; PD, co-culture supernatant with polydatin group. A phase contrast microscope was used to observe them. Typical microscopic fields are presented.

liver tissues from mice was investigated using WB and q-PCR, respectively. The protein expression levels of PCSK9 in mammary, lung, and liver tissues of tumor-bearing mice were significantly elevated compared to those of the control group. Moreover, HFD further increased the

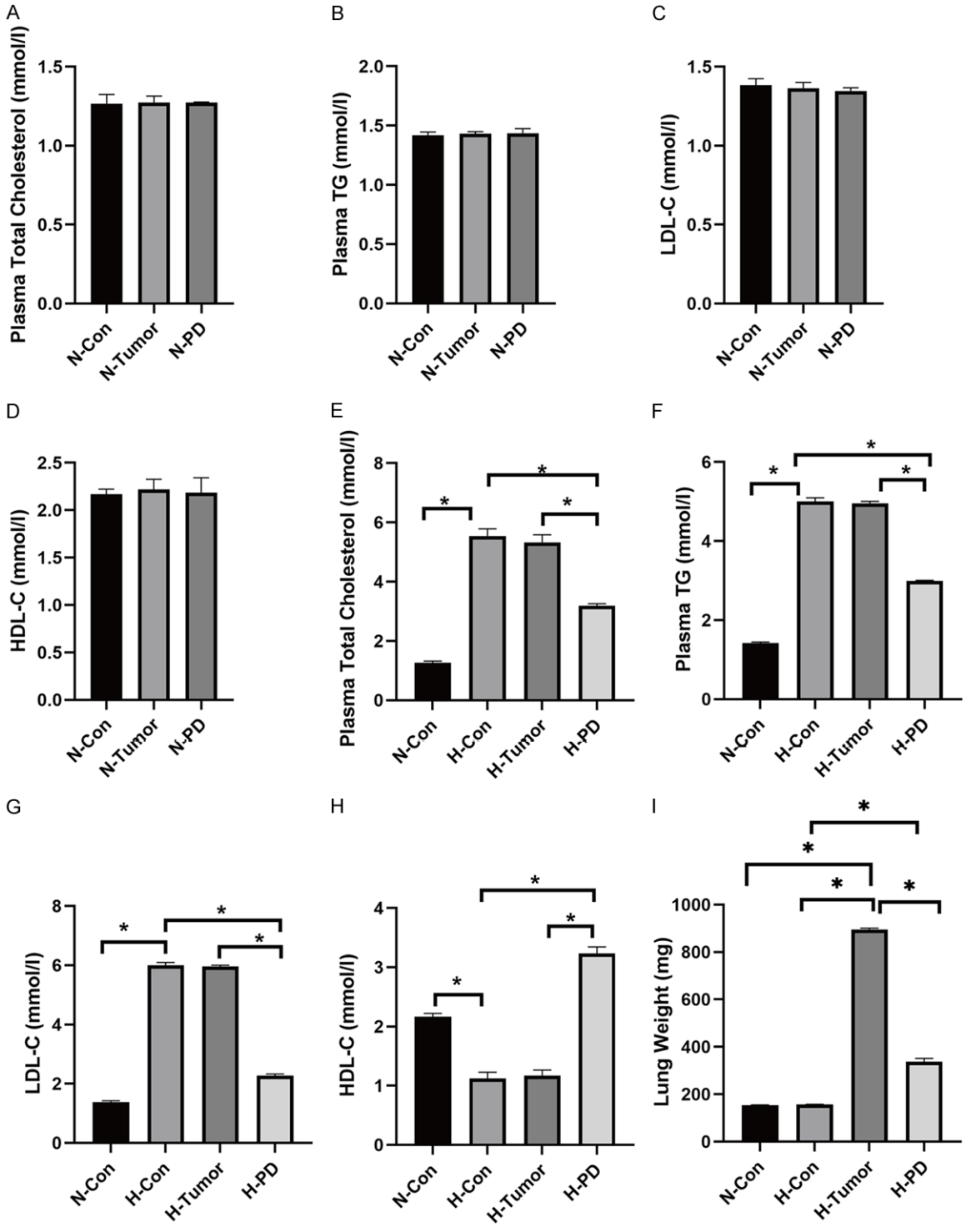

Figure 5. Polydatin therapy effects on total cholesterol (TC), triglyceride (TG), low-density lipoprotein cholesterol (LDL-C), and high-density lipoprotein cholesterol (HDL-C) in BALB/c mice receiving a regular chow diet or high-fat diet (HFD). A. The plasma TC. B. The plasma TG. C. The plasma LDL-C. D. The plasma HDL-C. E. The plasma TC. F. The plasma TG. G. The plasma LDL-C. H. The plasma HDL-C. I. Lung weight. *P<0.05. N-Con, a blank group with a standard chow diet; N-Tumor, tumor-bearing mice with a standard chow diet; N-PD, mice received polydatin therapy and fed with a standard chow diet; H-Con, a blank group administered HFD; H-Tumor, tumor-bearing mice administered HFD; H-PD, mice received polydatin therapy and administered HFD.

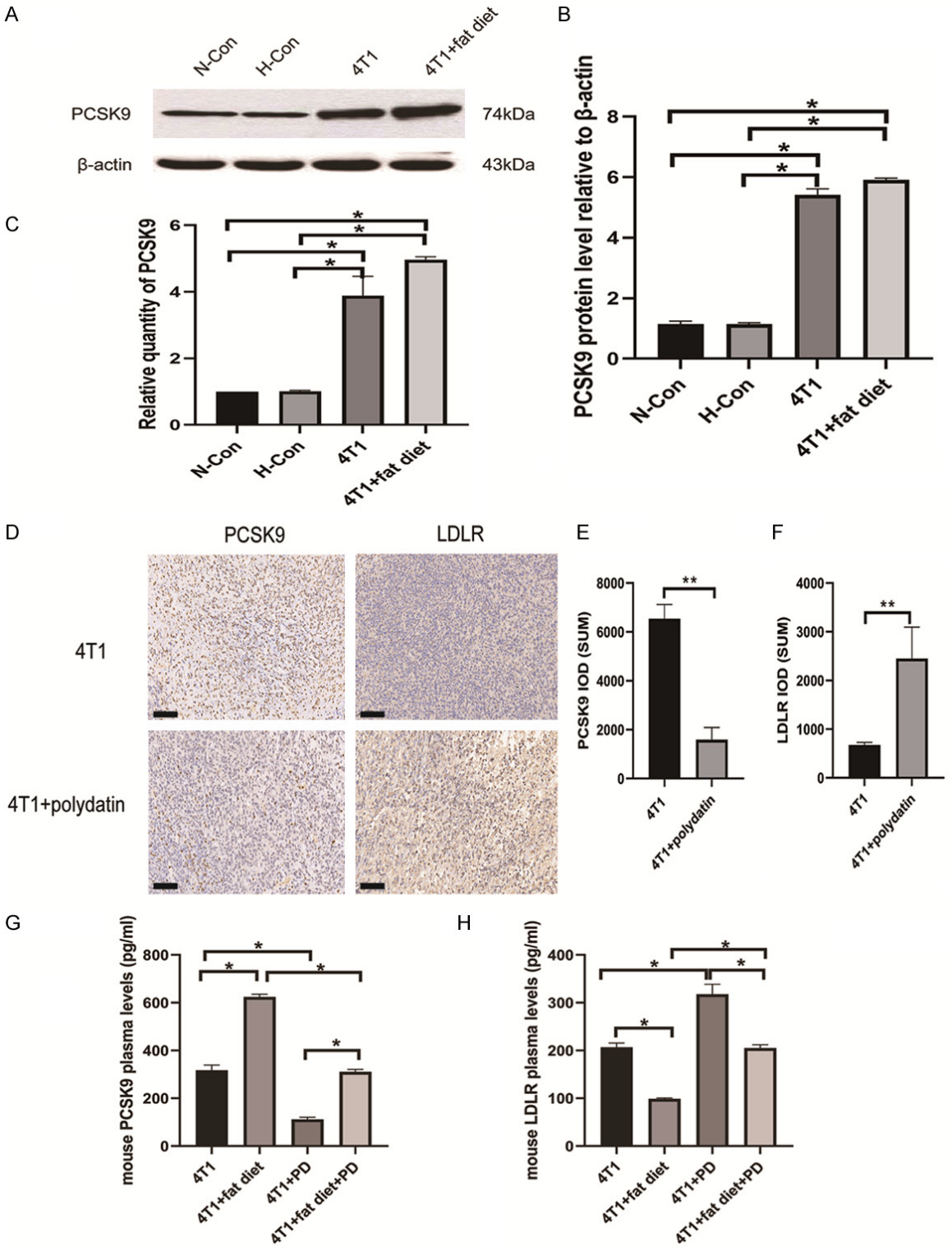

Figure 6. High-fat diet (HFD) and polydatin effects on mouse plasma and breast tumor tissue PCSK9 and LDLR expression. A. PCSK9 protein expression. B. Semi-quantitative analysis of PCSK9 protein. C. PCSK9 mRNA expression. All blots were subjected to scanning densitometry in triplicate, and the integrated optical density of each band was standardized to that of β-actin in the same blot. D. Immunohistochemical maps of PCSK9 and LDLR. In its original form, the magnification is ×100. E, F. Statistics of the positive number of PCSK9 and LDLR. G. Mouse PCSK9 plasma levels. H. Mouse LDLR plasma levels. *P<0.05, **P<0.01. H-Con, a blank group with an HFD; N-Con, a blank group with a conventional chow diet; 4T1, a tumor-bearing mice group fed a standard chow diet; 4T1+fat diet, a tumor-

bearing mice group on an HFD; 4T1+PD, a tumor-bearing mice group fed a standard chow diet and administered polydatin 100 mg/kg intraperitoneally every day; 4T1+fat diet+PD, a tumor-bearing mice group fed an HFD and administered polydatin 100 mg/kg intraperitoneally daily.

PCSK9 protein levels in these tissues, while polydatin treatment resulted in a significant decrease in PCSK9 expression. The expression of LDLR and PCSK9 exhibited an inverse correlation. The protein expression levels of LDLR in mammary, lung, and liver tissues of tumor-bearing mice were significantly lower compared to those of the control group. Additionally, HFD further reduced the LDLR protein levels of in these tissues. Conversely, treatment with polydatin resulted in a significant increase in the LDLR protein levels (**Figure 7A-G**). The mRNA expression of PCSK9 and LDLR exhibited concordant changes with the respective trends observed in their protein expression (**Figure 7H-M**).

The results suggest that the expression of PCSK9 is elevated in HFD-fed mice, and polydatin may enhance the expression of LDLR while inhibiting PCSK9 activity *in vivo.*

Polydatin suppressed the combination of PCSK9-LDLR and inhibited the expression of LDL-C in vitro

To investigate the role of polydatin in TNBC cells in a high-fat environment, we co-cultured 3T3-L1 and MDA-MB-231 cells with human normal mammary epithelial cell line (MCF-10A) *in vitro*. Compared with MCF-10A group, the protein level of PCSK9 in adipocyte cultured alone group (Adi) was slightly higher than that in MCF-10A group, but there was no statistical difference. The LDLR protein level in Adi group was nearly the same as that in MCF-10A group. The PCSK9 protein level in co-culture group (CAA) was significantly higher than that in the MCF-10A group, and the content of PCSK9 was 3.5 fold higher than that in MCF-10A group. Compared with MCF-10A group, the LDLR protein level was significantly decreased, and the content of LDLR was decreased by 87.1%. In co-culture system, the PCSK9 protein level in CAA+polydatin group was significantly decreased, and the content of PCSK9 was decreased by 53.1% compared with CAA group. The LDLR protein level was significantly increased, and its content was increased by 5.75 fold (**Figure 8A-C**).

q-PCR results showed that compared with MCF-10A group, the mRNA content of PCSK9 in Adi group was slightly higher than that in MCF-10A group, but the difference was not significant. The mRNA content of LDLR in Adi group was nearly the same as that in MCF-10A group. The mRNA content of PCSK9 in CAA group was significantly higher than that in MCF-10A group, and the content of PCSK9 was 4.95 fold higher than that in MCF-10A group. The mRNA content of LDLR was significantly lower that of MCF-10A group, and the LDLR content decreased by 59.8% compared with that of MCF-10A group. In co-culture system, the mRNA content of PCSK9 in CAA+polydatin group was significantly decreased by 49.8% compared with that in CAA group. The mRNA content of LDLR was increased by 2.32 fold (**Figure 8D**, **8E**).

PCSK9 can induce the degradation of LDLR, and then affect the expression of LDL-C. Therefore, WB and q-PCR were also carried out to measure the expression of LDL-C protein and mRNA in vitro. WB results showed that the LDL-C protein level in Adi group was almost similar to that in MCF-10A group, with no statistical difference. The LDL-C protein level in CAA group was significantly higher than that in MCF-10A group, and the content of LDL-C was 3.23 fold higher than that in MCF-10A group. Compared with CAA group, the protein level and content of LDL-C in the co-culture system (CAA+polydatin group) were significantly decreased by 80.9% (**Figure 8F**, **8H**).

q-PCR results showed that the mRNA content of LDL-C in Adi group was slightly higher than that in MCF-10A group, but there was no statistical difference. The LDL-C mRNA in CAA group was significantly higher than that in MCF-10A group, and the LDL-C content was 3.89 fold higher than that in MCF-10A group. In co-culture system, the LDL-C mRNA in CAA+polydatin group was significantly decreased by 51.2% when comparing with CAA group (**Figure 8G**).

PCSK9 played a role in reducing LDL-C in TNBC with a high-fat environment

Polydatin has been shown to decrease PCSK9 expression and reduce blood lipid phase and LDL-C expression levels. So, does PCSK9 play a role in LDL-C reduction? To transfect siRNAPC-

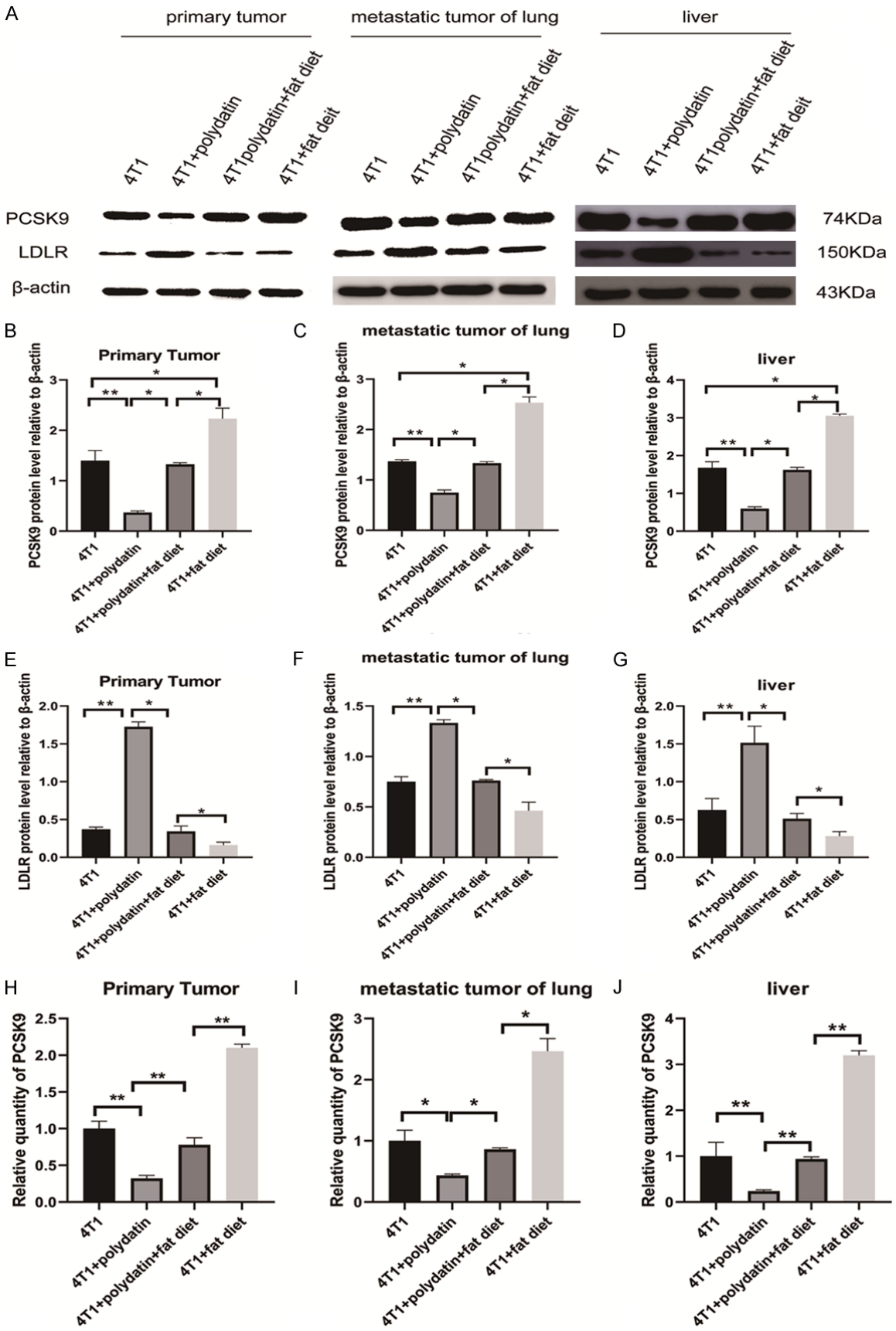
A
primary tumor
metastatic tumor of lung
liver
4T1
4T1+polydatin
4T1polydatin+fat diet
4T1+fat deit
PCSK9
LDLR
β-actin
74KDa
150KDa
43KDa
B
Primary Tumor
C
metastatic tumor of lung
D
liver
PCSK9 protein level relative to β-actin
E
Primary Tumor
F
metastatic tumor of lung
G
liver
LDLR protein level relative to β-actin
H
Primary Tumor
I
metastatic tumor of lung
J
liver
Relative quantity of PCSK9
4T1
4T1+polydatin
4T1+polydatin+fat diet
4T1+fat diet

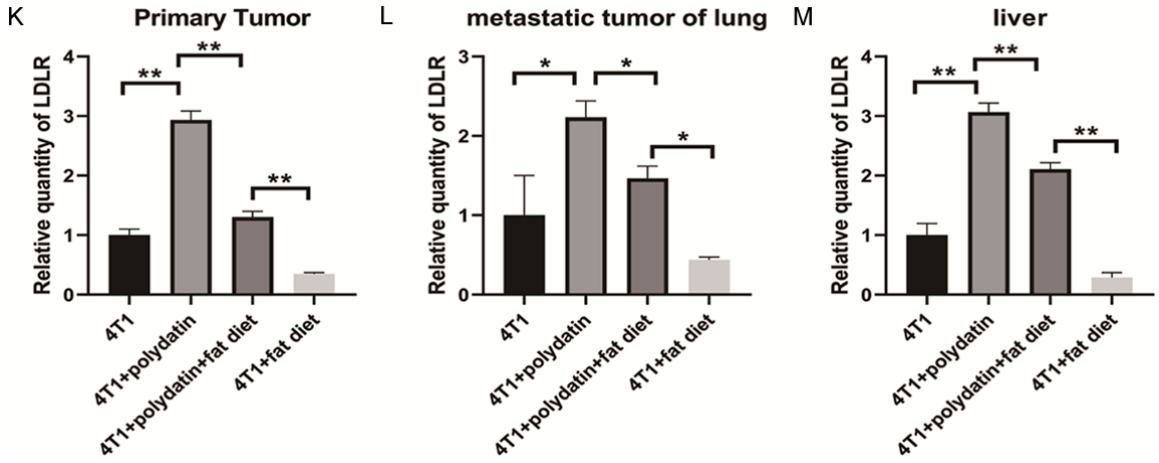

Figure 7. Changes in PCSK9 and LDLR protein and mRNA expression following polydatin treatment. A. PCSK9 and LDLR protein expression in 4T1, 4T1+fat diet, 4T1+polydatin+fat diet, and 4T1+polydatin treated primary tumor, lung, and liver tissues. B-D. Semi-quantitative analysis of PCSK9 protein. E-G. Semi-quantitative analysis of LDLR protein. All blots were subjected to scanning densitometry in triplicate, and the integrated optical density of each band was standardized to that of β-actin in the same blot. H-J. PCSK9 mRNA levels were measured in the primary tumor, lung, and liver tissues after treatment with 4T1, 4T1+fat diet-treated, 4T1+polydatin+fat diet, and 4T1+polydatin. K-M. Expression of LDLR mRNA in the primary tumor, lung, and liver tissues after treatment with 4T1, 4T1+fat diet-treated, 4T1+polydatin+fat diet, and 4T1+polydatin. *P<0.05, **P<0.01. 4T1, tumor-bearing mice fed regular chow; 4T1+ploydation, tumor-bearing mice on a conventional chow diet were administered polydatin 100 mg/kg intraperitoneally every day; 4T1+polydatin+fat diet, tumor-bearing mice on a high-fat diet (HFD) were administered polydatin 100 mg/kg intraperitoneally daily; 4T1+fat diet, tumor-bearing mice were fed with an HFD.

SK9 *in vitro*, we employed a co-culture system of adipocytes and TNBC cells. Protein expression of PCSK9 was reduced by 21.2% in the co-culture group following transfection with siRNAPCSK9, relative to the control group. In the control group, PCSK9 mRNA levels dropped by 11% (**Figure 9A-C**).

We conducted q-PCR to examine LDLR and LDL-C mRNA levels and WB to determine LDLR and LDL-C protein expression after transfecting co-cultured cells with siRNAPCSK9. Results showed that in the CAA group, LDLR mRNA expression increased 3.78-fold and LDLR protein expression increased 2.76-fold following PCSK9 knockdown. LDL-C mRNA expression dropped by 67% as compared to the CAA group. When compared to the CAA group, LDL-C protein expression decreased by 43%. After CAA treatment with polydatin, LDLR mRNA expression was 1.87-fold higher in the CAA+polydatin group than in the siRNAPCSK9 group. When compared to the siRNAPCSK9 group, LDLR protein level increased 1.84-fold. LDL-C mRNA expression was decreased by 76.2% compared to the siRNAPCSK9 group. In the siRNAPCSK9 group, LDL-C protein expression level was reduced by 42.1% (**Figure 9D-H**).

Overexpression of PCSK9 lentiviral vector (LV-PCSK9) was transfected into co-cultured cells in vitro. Following PCSK9 overexpression, the mRNA level of PCSK9 in co-culture cells rose 7.21 times compared to the CAA group; PCSK9 protein levels in co-culture cells were 3.1 times higher (**Figure 9I-K**). In co-culture cells (CAA), the LDLR mRNA level was reduced to 31% of that in the CAA group. In comparison to the CAA group, the LDLR protein level dropped to 46%. When compared to the CAA group, LDL-C mRNA expression rose by 2.7 times. Compared to CAA, LDL-C protein expression increased 1.8 times. After CAA+polydatin treatment, LDLR mRNA expression rose 3.42-fold compared to that of the CAA group. LDLR protein level increased 2.85 times when comparing with that in the CAA group. LDL-C protein expression was decreased by 63.1% when compared to the CAA group. These findings indicate that PCSK9 lowers LDL-C (**Figure 9L-P**).

Discussion

The prognosis for TNBC, one of the most prevalent malignancies in women, is among the poorest due to its highly aggressive nature [28-30]. The progression and prognosis of TNBC

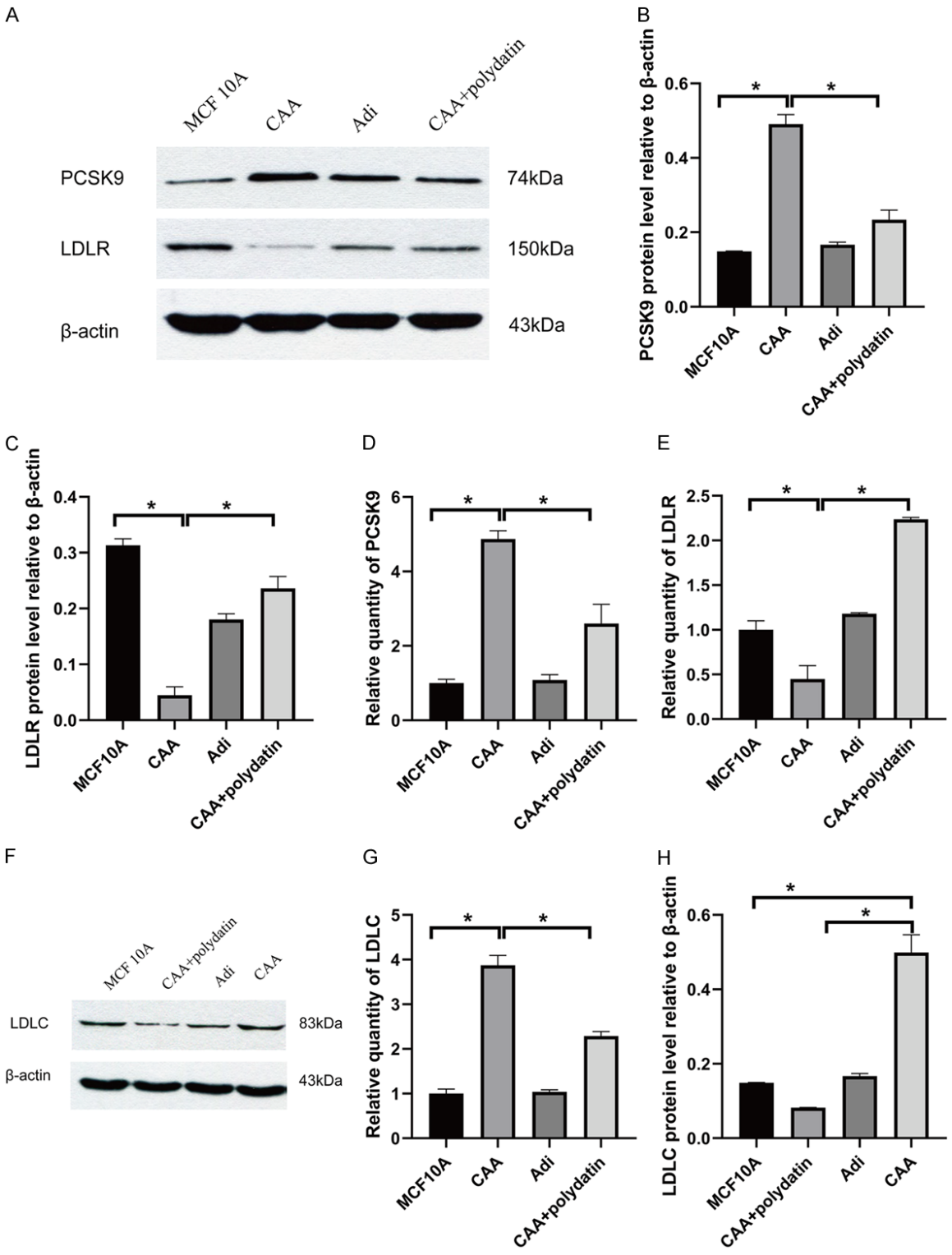

Figure 8. Polydatin suppressed the combination of PCSK9-LDLR and inhibited the expression of LDL-C *in vitro*. A. PCSK9 and LDLR protein expression in MCF-10A, CAA, Adi and CAA+polydatin. B. Semi-quantitative analysis of PCSK9 protein. C. Semi-quantitative analysis of LDLR protein. D. PCSK9 mRNA expression. E. LDLR mRNA expression. F. LDL-C protein expression in MCF-10A, CAA, Adi and CAA+polydatin. G. LDL-C mRNA expression. H. Semi-quantitative analysis of LDL-C protein. *P<0.05. MCF-10A, alone cultured human normal mammary epithelial cell line group; CAA, co-culture group; Adi, adipocyte cultured alone group; CAA+polydatin, co-cultured MDA-MB-231 and 3T3-L1 cells with polydatin into the co-culture system.

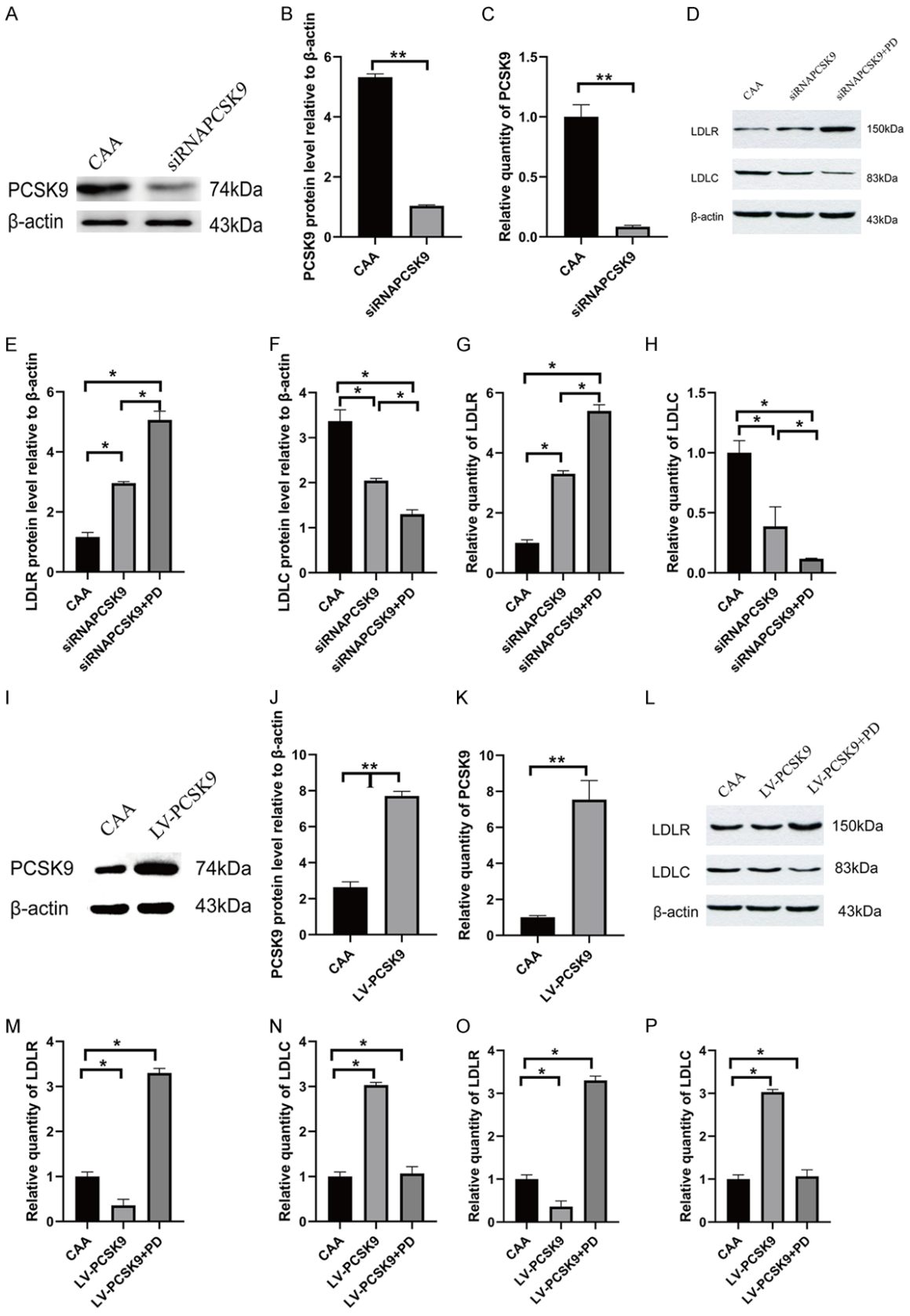

Figure 9. PCSK9 is implicated in reducing LDL-C in TNBC in a high-fat environment. A. PCSK9 protein expression in CAA and siRNAPCSK9. B. Semi-quantitative analysis of PCSK9 protein. C. PCSK9 mRNA expression. D. LDLR and

LDL-C protein expressions in CAA, siRNAPCSK9 and siRNAPCSK9+PD. E. Semi-quantitative analysis of LDLR protein. F. Semi-quantitative analysis of LDL-C protein. G. LDLR mRNA expression. H. LDL-C mRNA expression. I. PCSK9 protein expression in CAA and LV-PCSK9. J. Semi-quantitative analysis of PCSK9 protein. K. PCSK9 mRNA expression. L. LDLR and LDL-C protein expression in CAA, LV-PCSK9, and LV-PCSK9+PD. M. Semi-quantitative analysis of LDLR protein. N. Semi-quantitative analysis of LDL-C protein. O. LDLR mRNA expression. P. LDL-C mRNA expression.

are closely correlated with blood lipid levels [31, 32]. The LDL level serves as a significant indicator of tumor progression [33], particularly in relation to dyslipidemia. Furthermore, the association between dyslipidemia and overall survival in BC patients suggests its potential utility as a disease predictor [34-36]. At the same time, obesity has a direct impact on fat cell metabolism and poses a significant threat to the onset and progression of TNBC [37, 38]. PCSK9 has the ability to bind with LDLR for reducing LDL-C levels. Polydatin represents a novel herbal anticancer medication that exhibits efficacy in treating various diseases, including BC associated with hyperlipidemia [39]. Many studies have found a correlation between PCSK9 overexpression and hypercholesterolemia and multiple cancers [40, 41]. An experimental model has revealed possible anti-BC effects of the anti-PCSK9 vaccination [42]. BC cells have a higher cholesterol proportion and many of them overexpress PCSK9 than normal human mammary epithelial cells [43]. Cholesterol-rich diets were found to significantly increase BC metastasis in experiments on animals [44]. However, PCSK9 inhibitors have not been examined concerning hypercholesterolemia-induced TNBC growth and metastasis. Additionally, it is unclear how polydatin affects PCSK9 and LDLR expression, and there have been no studies of PCSK9 in TNBC to date. Thus, PCSK9 attracted our interest, and we logically hypothesized that polydatin would increase LDLR expression in TNBC by decreasing PCSK9 levels. This effect may reduce the risk of TNBC associated with dyslipidemia, which increases LDLR levels while decreasing LDL-C levels to counterbalance hyperglycemia. Both *in vitro* and *in vivo* investigations were designed for demonstrating our hypothesis.

The present study utilized the co-culture of the MDA-MB-231 and 3T3-L1 cell lines to investigate polydatin's anticancer activity *in vivo*. This method was selected because of polydatin's capacity to mimic the adipose milieu, in which MDA-MB-231 cells overexpress PCSK9. According to our findings, polydatin was shown to significantly suppress TNBC proliferation and migration, as well as decrease PCSK9 expression in co-cultured adipocytes and pre-adipocytes. Additionally, adipocytes were more successful than pre-adipocytes in enhancing BC cell development; nevertheless, more study is needed to demonstrate that both pre-adipocytes and adipocytes may enhance BC cell migration. Growth and migration of tumor cells are essential features of tumorigenesis. The effects of polydatin on MDA-MB-231 cell proliferation and migration were investigated in a co-culture model. Our results imply that polydatin acted as a PCSK9 inhibitor, as it decreased both the proliferation and migration in the co-culture system. We observed an upregulation of PCSK9 and a downregulation of LDLR in the co-culture system. Based on these results, we hypothesized that PCSK9 may act as a tumor promoter in the co-culture system and that polydatin could raise LDLR levels by suppressing PCSK9 expression and blocking the coupling of PCSK9 and LDLR. To test the aforementioned hypotheses, a siRNA and PCSK9 lentiviral vector transfection assay was performed. In the SiRNAPCSK9+PD group, polydatin-induced enhancement of LDLR expression was observed. In the co-culture system, when PCSK9 was overexpressed relative to the empty vector group, LDLR levels decreased remarkably. Polydatin is implicated in PCSK9-mediated modulation of LDLR and LDL-C, according to these findings.

We also used an HFD model with TNBC to further express our point of view. Our earlier investigation found a link between HFD and an aggressive TNBC phenotype [27]. In a mouse model of BC, 4T1-luc cell tumors progressed faster in mice fed an HFD (11% fat content) than in animals fed a regular diet (5% fat content). Tumor tissue from HFD-fed mice showed increased PCSK9 and LDLR expression and differentiation compared to tumor tissue from chow-fed mice, as determined using IHC analysis. Therefore, HFD was used in all subsequent *in vivo* assays. Our findings further showed that polydatin therapy significantly suppressed

4T1-luc tumor growth in both the breast tumor-bearing mice and the tail vein metastasis models, compared to vehicle control. Consistent with the prior study findings, the polydatin treatment group exhibited substantial lipid-lowering effects [27]. PCSK9 protein and mRNA levels increased in HFD model TNBC primary tumor tissue, lung metastatic tumor tissue, and liver tissue. LDLR mRNA and protein levels were lower in metastatic lung tumor tissue, primary tumor tissue, and liver tissue. After polydatin exposure, LDLR levels increased, whereas PCSK9 mRNA and protein levels decreased in TNBC mice model fed with HFD. Many studies have demonstrated the physiological significance of PCSK9's activity as a secreted factor [45, 46]. Hence, we investigated polydatin-influenced serum PCSK9 levels. Using ELISA, we determined that polydatin inhibited PCSK9 and raised LDLR levels in serum. Our findings suggest that polydatin improves LDL-C and lipid metabolism by suppressing PCSK9 in TNBC with hyperlipidemia, and they support the idea of targeting the PCSK9 pathway as a new method to regulate TNBC progression. However, our study also has certain limitations, such as the need for further investigation into the regulatory pathway of polydatin on PCSK9 and the validation of PCSK9 in other subtypes of BC. Additionally, we plan to collect clinical samples in future studies to verify these findings specifically in the TNBC population, which will enhance the credibility of our experimental results.

Conclusions

The findings of this study suggest that polydatin inhibits lipid metabolism and lowers LDL-C content via a mechanism that is strongly related to suppressing PCSK9. Our findings offer a new foundation for future clinical research into the therapeutic potentials of polydatin among individuals with TNBC and hyperlipidemia.

Acknowledgements

This study was funded by Enshi Prefecture Science and Technology Program Research and Development Project (No. JCY2019000-040).

Disclosure of conflict of interest

None.

Address correspondence to: Qing Zhang, Department of Oncology, Beijing Hospital of Traditional Chinese Medicine, Capital Medical University, No. 23 Meishuguanhou Street, Dongcheng District, Beijing 100010, China. Tel: +86-01052176934; E-mail: zhangqing@ccmu.edu.cn

References

[1] Sung H, Ferlay J, Siegel RL, Laversanne M, Soerjomataram I, Jemal A and Bray F. Global cancer statistics 2020: GLOBOCAN estimates of incidence and mortality worldwide for 36 cancers in 185 countries. CA Cancer J Clin 2021; 71: 209-249.

[2] Lengyel E, Makowski L, DiGiovanni J and Kolonin MG. Cancer as a matter of fat: the crosstalk between adipose tissue and tumors. Trends Cancer 2018; 4: 374-384.

[3] Picon-Ruiz M, Morata-Tarifa C, Valle-Goffin JJ, Friedman ER and Slingerland JM. Obesity and adverse breast cancer risk and outcome: mechanistic insights and strategies for intervention. CA Cancer J Clin 2017; 67: 378-397.

[4] Santander AM, Lopez-Ocejo O, Casas O, Agostini T, Sanchez L, Lamas-Basulto E, Carrio R, Cleary MP, Gonzalez-Perez RR and Torroella-Kouri M. Paracrine interactions between adipocytes and tumor cells recruit and modify macrophages to the mammary tumor microenvironment: the role of obesity and inflammation in breast adipose tissue. Cancers (Basel) 2015; 7: 143-178.

[5] Pires LA, Hegg R, Freitas FR, Tavares ER, Almeida CP, Baracat EC and Maranhão RC. Effect of neoadjuvant chemotherapy on low-density lipoprotein (LDL) receptor and LDL receptor-related protein 1 (LRP-1) receptor in locally advanced breast cancer. Braz J Med Biol Res 2012; 45: 557-564.

[6] Gallagher EJ, Zelenko Z, Neel BA, Antoniou IM, Rajan L, Kase N and LeRoith D. Elevated tumor LDLR expression accelerates LDL cholesterol-mediated breast cancer growth in mouse models of hyperlipidemia. Oncogene 2017; 36: 6462-6471.

[7] Lu CW, Lo YH, Chen CH, Lin CY, Tsai CH, Chen PJ, Yang YF, Wang CH, Tan CH, Hou MF and Yuan SF. VLDL and LDL, but not HDL, promote breast cancer cell proliferation, metastasis and angiogenesis. Cancer Lett 2017; 388: 130-138.

[8] dos Santos CR, Domingues G, Matias I, Matos J, Fonseca I, de Almeida JM and Dias S. LDL-cholesterol signaling induces breast cancer proliferation and invasion. Lipids Health Dis 2014; 13: 16.

[9] Deng CF, Zhu N, Zhao TJ, Li HF, Gu J, Liao DF and Qin L. Involvement of LDL and ox-LDL in cancer development and its therapeutical potential. Front Oncol 2022; 12: 803473.

[10] Derakhshan F and Reis-Filho JS. Pathogenesis of triple-negative breast cancer. Annu Rev Pathol 2022; 17: 181-204.
[11] Banerjee Y, Santos RD, Al-Rasadi K and Rizzo M. Targeting PCSK9 for therapeutic gains: have we addressed all the concerns. Atherosclerosis 2016; 248: 62-75.
[12] El Khoury P, Elbitar S, Ghaleb Y, Khalil YA, Varret M, Boileau C and Abifadel M. PCSK9 mutations in familial hypercholesterolemia: from a groundbreaking discovery to anti-PCSK9 therapies. Curr Atheroscler Rep 2017; 19: 49.
[13] Wang Y and Liu ZP. PCSK9 inhibitors: novel therapeutic strategies for lowering LDLCholesterol. Mini Rev Med Chem 2019; 19: 165-176.
[14] Abdelwahed KS, Siddique AB, Mohyeldin MM, Qusa MH, Goda AA, Singh SS, Ayoub NM, King JA, Jois SD and El Sayed KA. Pseurotin A as a novel suppressor of hormone dependent breast cancer progression and recurrence by inhibiting PCSK9 secretion and interaction with LDL receptor. Pharmacol Res 2020; 158: 104847.
[15] Lv R, Du L, Liu X, Zhou F, Zhang Z and Zhang L. Polydatin alleviates traumatic spinal cord injury by reducing microglial inflammation via regulation of iNOS and NLRP3 inflammasome pathway. Int Immunopharmacol 2019; 70: 28-36.
[16] Zhao L, Liu H, Wang Y, Wang S, Xun D, Wang Y, Cheng Y and Zhang B. Multimodal identification by transcriptomics and multiscale bioassays of active components in Xuanfeibaidu formula to suppress macrophage-mediated immune response. Engineering (Beijing) 2023; 20: 63-76.
[17] Peritore AF, D'Amico R, Cordaro M, Siracusa R, Fusco R, Gugliandolo E, Genovese T, Crupi R, Di Paola R, Cuzzocrea S and Impellizzeri D. PEA/polydatin: anti-inflammatory and antioxidant approach to counteract DNBS-induced colitis. Antioxidants (Basel) 2021; 10: 464.
[18] Chen G, Yang Z, Wen D, Guo J, Xiong Q, Li P, Zhao L, Wang J, Wu C and Dong L. Polydatin has anti-inflammatory and antioxidant effects in LPS-induced macrophages and improves DSS-induced mice colitis. Immun Inflamm Dis 2021; 9: 959-970.
[19] Li Z, Chen X, Liu G, Li J, Zhang J, Cao Y and Miao J. Antioxidant activity and mechanism of resveratrol and polydatin isolated from mulberry (Morus alba L.). Molecules 2021; 26: 7574.
[20] Yang B, Li JJ, Cao JJ, Yang CB, Liu J, Ji QM and Liu ZG. Polydatin attenuated food allergy via store-operated calcium channels in mast cell. World J Gastroenterol 2013; 19: 3980-3989.
[21] Jiang CQ, Ma LL, Lv ZD, Feng F, Chen Z and Liu ZD. Polydatin induces apoptosis and autophagy via STAT3 signaling in human osteosarcoma MG-63 cells. J Nat Med 2020; 74: 533-544.
[22] Yang Y, Zhang G, Li C, Wang S, Zhu M, Wang J, Yue H, Ma X, Zhen Y and Shu X. Metabolic profile and structure-activity relationship of resveratrol and its analogs in human bladder cancer cells. Cancer Manag Res 2019; 11: 4631-4642.
[23] Hu T, Fei Z, Su H, Xie R and Chen L. Polydatin inhibits proliferation and promotes apoptosis of doxorubicin-resistant osteosarcoma through LncRNA TUG1 mediated suppression of Akt signaling. Toxicol Appl Pharmacol 2019; 371: 55-62.
[24] Verma N and Tiku AB. Polydatin-induced direct and bystander effects in A549 lung cancer cell line. Nutr Cancer 2022; 74: 237-249.
[25] Ahmad P, Alvi SS, Iqbal D and Khan MS. Insights into pharmacological mechanisms of polydatin in targeting risk factors-mediated atherosclerosis. Life Sci 2020; 254: 117756.
[26] Liu W, Chen P, Deng J, Lv J and Liu J. Resveratrol and polydatin as modulators of Ca(2+) mobilization in the cardiovascular system. Ann N Y Acad Sci 2017; 1403: 82-91.
[27] Liu M, Li Y, Kong B, Zhang G and Zhang Q. Polydatin down-regulates the phosphorylation level of STAT3 and induces pyroptosis in triple-negative breast cancer mice with a high-fat diet. Ann Transl Med 2022; 10: 173.
[28] Vagia E, Mahalingam D and Cristofanilli M. The landscape of targeted therapies in TNBC. Cancers (Basel) 2020; 12: 916.
[29] Hoy AJ, Balaban S and Saunders DN. Adipocyte-tumor cell metabolic crosstalk in breast cancer. Trends Mol Med 2017; 23: 381-392.
[30] Loibl S, Turner NC, Ro J, Cristofanilli M, Iwata H, Im SA, Masuda N, Loi S, André F, Harbeck N, Verma S, Folkerd E, Puyana Theall K, Hoffman J, Zhang K, Bartlett CH and Dowsett M. Palbociclib combined with fulvestrant in premenopausal women with advanced breast cancer and prior progression on endocrine therapy: PALOMA-3 results. Oncologist 2017; 22: 1028-1038.
[31] Yadav NK, Poudel B, Thanpari C and Chandra Koner B. Assessment of biochemical profiles in premenopausal and postmenopausal women with breast cancer. Asian Pac J Cancer Prev 2012; 13: 3385-3388.
[32] Owiredu WK, Donkor S, Addai BW and Amidu N. Serum lipid profile of breast cancer patients. Pak J Biol Sci 2009; 12: 332-338.
[33] Chang SJ, Hou MF, Tsai SM, Wu SH, Hou LA, Ma H, Shann TY, Wu SH and Tsai LY. The association between lipid profiles and breast cancer among Taiwanese women. Clin Chem Lab Med 2007; 45: 1219-1223.
[34] Furberg AS, Jasienska G, Bjurstam N, Torjesen PA, Emaus A, Lipson SF, Ellison PT and Thune

I. Metabolic and hormonal profiles: HDL cholesterol as a plausible biomarker of breast cancer risk. The Norwegian EBBA Study. Cancer Epidemiol Biomarkers Prev 2005; 14: 33-40.
[35] Zhao X, Guo X, Jiao D, Zhu J, Xiao H, Yang Y, Zhao S, Zhang J, Jiao F and Liu Z. Analysis of the expression profile of serum exosomal lncRNA in breast cancer patients. Ann Transl Med 2021; 9: 1382.
[36] Emaus A, Veierød MB, Tretli S, Finstad SE, Selmer R, Furberg AS, Bernstein L, Schlichting E and Thune I. Metabolic profile, physical activity, and mortality in breast cancer patients. Breast Cancer Res Treat 2010; 121: 651-660.
[37] Sun H, Zou J, Chen L, Zu X, Wen G and Zhong J. Triple-negative breast cancer and its association with obesity. Mol Clin Oncol 2017; 7: 935-942.
[38] Hossain F, Majumder S, David J, Bunnell BA and Miele L. Obesity modulates the gut microbiome in triple-negative breast cancer. Nutrients 2021; 13: 3656.
[39] Canuel M, Sun X, Asselin MC, Paramithiotis E, Prat A and Seidah NG. Proprotein convertase subtilisin/kexin type 9 (PCSK9) can mediate degradation of the low density lipoprotein receptor-related protein 1 (LRP-1). PLoS One 2013; 8: e64145.
[40] Sun X, Essalmani R, Day R, Khatib AM, Seidah NG and Prat A. Proprotein convertase subtilisin/kexin type 9 deficiency reduces melanoma metastasis in liver. Neoplasia 2012; 14: 1122-1131.
[41] Athavale D, Chouhan S, Pandey V, Mayengbam SS, Singh S and Bhat MK. Hepatocellular carcinoma-associated hypercholesterolemia: involvement of proprotein-convertase-subtilisin-kexin type-9 (PCSK9). Cancer Metab 2018; 6: 16.
[42] Momtazi-Borojeni AA, Nik ME, Jaafari MR, Banach M and Sahebkar A. Effects of immunization against PCSK9 in an experimental model of breast cancer. Arch Med Sci 2019; 15: 570-579.
[43] Buss LA and Dachs GU. The role of exercise and hyperlipidaemia in breast cancer progression. Exerc Immunol Rev 2018; 24: 10-25.
[44] Gu J, Zhu N, Li HF, Zhao TJ, Zhang CJ, Liao DF and Qin L. Cholesterol homeostasis and cancer: a new perspective on the low-density lipoprotein receptor. Cell Oncol (Dordr) 2022; 45: 709-728.
[45] Grefhorst A, McNutt MC, Lagace TA and Horton JD. Plasma PCSK9 preferentially reduces liver LDL receptors in mice. J Lipid Res 2008; 49: 1303-1311.
[46] Baass A, Dubuc G, Tremblay M, Delvin EE, O'Loughlin J, Levy E, Davignon J and Lambert M. Plasma PCSK9 is associated with age, sex, and multiple metabolic markers in a population-based sample of children and adolescents. Clin Chem 2009; 55: 1637-1645.